

EXTRUDATE SWELL FOR A ROUND JET WITH LARGE SURFACE TENSION

H.A. TIEU and D.D. JOSEPH

Department of Aerospace Engineering and Mechanics, University of Minnesota, Minneapolis, Minnesota 55455 (U.S.A.)

(Received February 10, 1983)

Summary

The problem of extrudate swell of a viscoelastic fluid from a round pipe is studied by the method of domain perturbations. The perturbation problems are solved by a finite-element method through second-order in the flow rate parameter ϵ for small flow rates. The analysis extends the work of Sturges on swelling in two-dimensional channels to round capillary tubes. In perturbation studies for small ϵ , the rheology of the fluid may be expressed by three parameters, the viscosity and the two constants α_1 and α_2 appearing at order two in the expansion of the extra stress around zero shear. Surface tension has an important influence on the shape of the jet at low speeds. The shape of the surface on a round jet depends on α_1 and α_2 , in the plane jet only on α_1 . The analysis predicts that no matter what the constitutive equation may be, the jet will first contract if the radius of the pipe is sufficiently small. The contraction takes place in a length less than $1/10$ the diameter of the jet and is followed by a swell. The contraction is usually small and may be hard to observe. There are five different contributions to the jet shape at second-order but only the viscoelastic ones persist as the pipe radius goes to zero.

1. Introduction and conclusion

An incompressible fluid tends to deform its free boundary laterally outward as it exits from a conduit at low Reynolds numbers. This so called extrudate swell phenomenon has been a controversial topic and has attracted the attention of many rheologists. Theoretically, one may analyse the problem by either numerical simulations or analytical methods. Due to the complex nature of the problem (e.g., mixed boundary data), much of the

research effort has relied on numerical methods. A complete survey on these numerical analysis is, however, outside the scope of this paper. Readers interested in this domain of the subject are referred to a recent paper by Crochet and Keunings [1], in which the authors assumed zero surface tension and an upper convected Maxwell model for the fluid, and were able to obtain swell ratio as high as 100%. On the other hand, analytical approaches to the problem are centered about either overall conservation laws (e.g., Joseph [3]) or perturbation methods. Applications of the latter have been recently illustrated through second order in the plane jet (Sturges [2]), and in the linearized problem of the round jet (Trogdon and Joseph [4,5]).

Our analysis is very close to the one by Sturges [2]. He studied the problem of extrudate swell of a plane jet using the method of domain perturbations and calculated solutions through second-order analytically, using biorthogonal series. Here, we study the round jet and use finite elements to compute the perturbation solutions through second order. The perturbation method can be more or less general than numerical studies using explicit rheological models. It is less general because it applies only to problems which in some sense perturb a state of rest. It is more general because the rheology of the fluid at low shears can be characterized by a few constants, no matter how complicated the underlying constitutive equation may be supposed to be.

Our results, like our methods, are close to the ones exhibited by Sturges except that in the axisymmetric case we get an extra term, zero in the plane, which involves not only the zero shear limit $-2\alpha_1$ of the first normal stress difference coefficient but also the zero shear limit $2\alpha_1 + \alpha_2$ of the second normal stress difference. Another way to say the foregoing is that the swell at second order in plane flow depends on non-Newtonian contributions of the form

$$\lim_{x \rightarrow 0} \frac{N_1(x)}{x^2} = -2\alpha_1.$$

Terms which prevent the proof of Tanner's theorem in the axisymmetric case bring extra terms proportional to α_2 into the expressions for the motion and the free surface.

In this paper, we shall give the equations which we solved by finite elements. We shall discuss the shape of the free surface. Detailed graphs of pressure and velocity distributions of the perturbation problems can be found in Tieu's Thesis [7]. We tried to compare our solution with experiments but we failed because there are no systematic experiments showing the dependence of the jet shape at low speeds under conditions in which the controlling parameters and the (important) pipe radius are varied systemati-

cally. There are many photographs of extrudate swell in the published literature but they are all casual.

We now complete the introduction by stating the main results of our analysis and computations.

We have derived the following expression for the shape of the jet

$$\begin{aligned} \frac{h(x)}{a} = 1 + \frac{\mu\bar{u}}{\sigma} \left[\frac{\hat{h}_1(\hat{x})}{2} \right] + \frac{\rho a \bar{u}^2}{\sigma} \left[\frac{\hat{h}_{20}(\hat{x})}{4} \right] + \frac{\alpha_1 \bar{u}^2}{a\sigma} \left[\frac{\hat{h}_{21}(\hat{x})}{4} \right] \\ + \frac{\alpha_2 \bar{u}^2}{a\sigma} \left[\frac{\hat{h}_{22}(\hat{x})}{4} \right] + \left(\frac{\mu\bar{u}}{\sigma} \right)^2 \left[\frac{\hat{h}_{23}(\hat{x})}{4} \right] + O(|\bar{u}|^3), \end{aligned} \quad (1.1)$$

where (see Fig. 1): $\hat{x} = x/a$, and $h(x)$, a , \bar{u} denote the jet shape, the pipe radius and the average velocity of the flow respectively, ρ and σ are the density and the surface tension of the fluid, μ and α_1 , α_2 the viscosity and viscoelastic material constants which appear in expression (2.4) of the extra stress in a second grade fluid. The functions $\hat{h}_i(\hat{x})$ and $\hat{h}_{2i}(\hat{x})$ with $i = 0, 1, 2, 3$, are parameter-free functions determined as solutions of the boundary value problems in Section 2. The graphs of the functions are displayed in Figs. 2–6. We note that the functions $\hat{h}_i(\hat{x})$, $\hat{h}_{2i}(\hat{x})$, $i = 0, 1, 2$, already attain at $\hat{x} = 2$ their corresponding asymptotic values at $\hat{x} = +\infty$, whereas $\hat{h}_{23}(2)$ is about 10% less in magnitude than its asymptotic value. Our solution (1.1) is therefore completely explicit with regard to its dependence on the parameters and it gives the shape of the jet, as well as its final radius.

For very small capillary tubes, (1.1) reduces to

$$h(x) = a + \frac{\alpha_1 \bar{u}^2}{\sigma} \left[\frac{\hat{h}_{21}(\hat{x})}{4} \right] + \frac{\alpha_2 \bar{u}^2}{\sigma} \left[\frac{\hat{h}_{22}(\hat{x})}{4} \right] + O(a). \quad (1.2)$$

This shows how the effects of viscoelasticity are amplified in small tubes.

The solution (1.1) can be compared with the expression

$$\begin{aligned} \frac{h(x)}{b} = 1 + \frac{\mu\bar{u}}{\sigma} [2\hat{h}_{1r}(\hat{x})] + \frac{\rho b \bar{u}^2}{\sigma} [4\hat{h}_{mi}(\hat{x})] + \frac{\alpha_1 \bar{u}^2}{b\sigma} [4\hat{h}_{sg}(\hat{x})] \\ + \left(\frac{\mu\bar{u}}{\sigma} \right)^2 [4\hat{h}_{mb}(\hat{x})] + O(|\bar{u}|^3), \end{aligned} \quad (1.3)$$

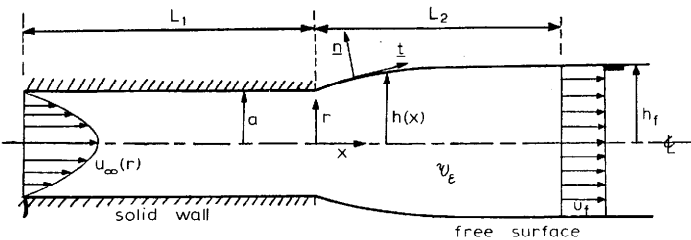


Fig. 1. Extrudate swell.

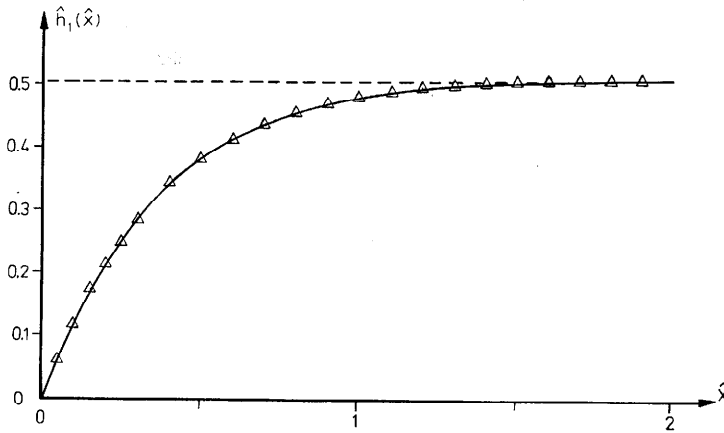


Fig. 2. Surface shape correction at first order, determined from problem (2.29–36). Results computed on Meshes I–IV are essentially the same. Mesh I \square ; Mesh II \times ; Mesh III \circ ; Mesh IV \triangle .

given by Sturges for the plane jet. (The numerical coefficients in the brackets of (1.3) are different from those in (1.1) because the perturbation parameter ϵ in Sturges' analysis is not the same as ours (2.13)). The viscoelastic contribution to the plane jet has no term proportional to α_2 .

It is well known that α_2 is a parameter associated with nonlinear viscous

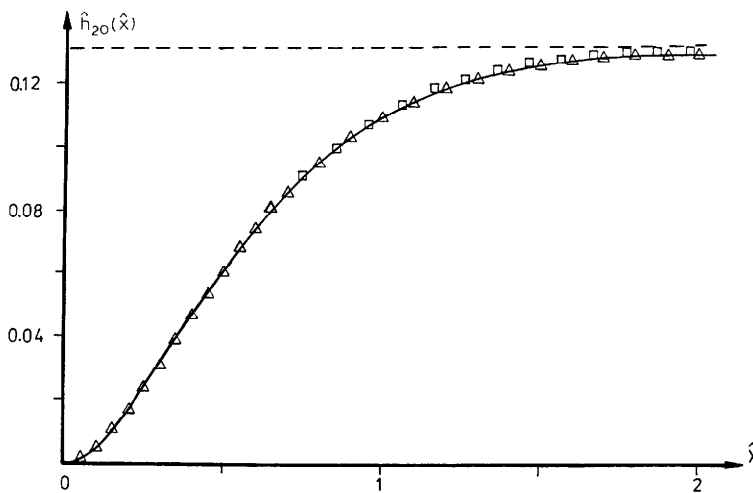


Fig. 3. Surface shape correction at second order due to Reynolds number, determined from problem (2.56.A–B). See legend of Fig. 2. Results computed on Meshes I–IV are very close together.

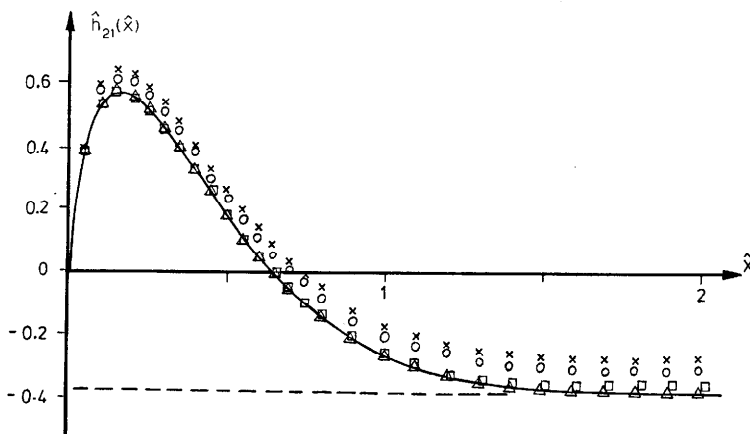


Fig. 4. Surface shape correction at second order due to α_1 , determined from problem (2.57.A–B). See legend of Fig. 2.

fluids which do not exhibit elastic behavior (Reiner–Rivlin fluids). The dependence of the jet radius on α_2 therefore contradicts the notion that the jet swell is determined by elastic recovery and returns a little to the original conjectures of Reiner about the normal stress contribution to the swell (see Truesdell and Noll [8]).

It is generally assumed that polymeric fluids will climb rods (Weissenberg effect). This implies that $3\alpha_1 + 2\alpha_2 > 0$ (Joseph and Fosdick [9]). On the other hand, the polymeric fluids for which values of the second normal stress difference have been reported are such that $2\alpha_1 + \alpha_2 < 0$. It then follows (Saut and Joseph [10]) that there is a $C \in [1, \frac{4}{3}]$ such that for each climbing fluid with a limiting negative second normal stress difference $2\alpha_1 + C\alpha_2 = 0$.

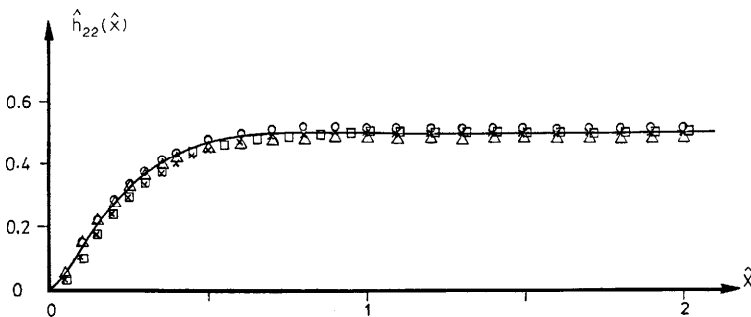


Fig. 5. Surface shape correction at second order due to α_2 , determined from problem (2.58.A–B). See legend of Fig. 2.

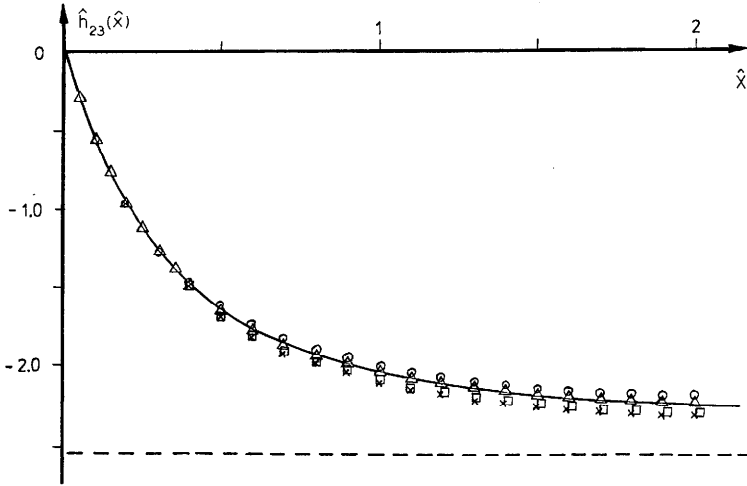


Fig. 6. Surface shape correction at second order, determined from problem (2.59.A–B). See legend of Fig. 2.

Using this relation, we may rewrite (1.1):

$$\begin{aligned} \frac{h(x)}{a} = & 1 + \frac{\mu\bar{u}}{\sigma} \left[\frac{\hat{h}_1(\hat{x})}{2} \right] + \frac{\rho a \bar{u}^2}{\sigma} \left[\frac{\hat{h}_{20}(\hat{x})}{4} \right] + \frac{\alpha \hat{u}^2}{a\sigma} \frac{1}{4} \left[\hat{h}_{21}(\hat{x}) - \frac{2}{C} \hat{h}_{22}(\hat{x}) \right] \\ & + \left(\frac{\mu\hat{u}}{\sigma} \right)^2 \left[\frac{\hat{h}_{23}(\hat{x})}{4} \right] + O(|\bar{u}|^3). \end{aligned} \tag{1.4}$$

We may also introduce dimensionless parameters

$$w_e = -\frac{\alpha_1 \bar{u}}{2a\mu}, \quad R_e \equiv \frac{2\rho a \bar{u}}{\mu}, \quad \kappa \equiv \frac{2\mu\bar{u}}{\sigma}.$$

In terms of these dimensionless parameters, (1.4) can be written as

$$\begin{aligned} \frac{h(x)}{a} = & 1 + \kappa \left[\frac{\hat{h}_1(\hat{x})}{4} + R_e \frac{\hat{h}_{20}(\hat{x})}{16} + w_e \left(\frac{\hat{h}_{22}(\hat{x})}{2C} - \frac{\hat{h}_{21}(\hat{x})}{4} \right) \right] \\ & + \kappa^2 \frac{\hat{h}_{23}(\hat{x})}{16} + O(|\bar{u}|^3). \end{aligned} \tag{1.5}$$

The viscoelastic effects on the jet shape are exhibited by the functions

$$\hat{h}_{NN}(\hat{x}) \equiv \frac{\hat{h}_{22}(\hat{x})}{2C} - \frac{\hat{h}_{21}(\hat{x})}{4}.$$

The viscoelastic contributions are therefore bounded between two limiting cases $C = 1$ and $4/3$, which are shown in Fig. 7. We note in this figure that $\hat{h}_{NN}(\hat{x})$ attains its minimum at $\hat{x}_t \approx 0.06$ and $\hat{h}_{NN}(\hat{x}_t) \approx -0.1$. The condition

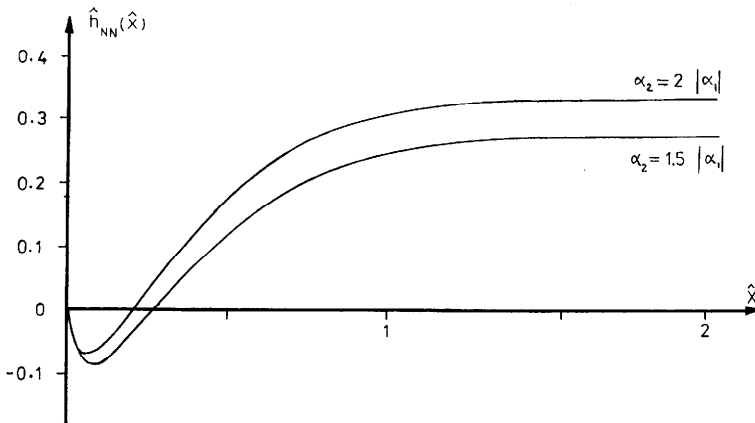


Fig. 7. Surface shape correction at second order due to viscoelasticity in a fluid.

$$\hat{h}_{NN}(\hat{x}) = \frac{\hat{h}_{22}(\hat{x})}{2C} - \frac{\hat{h}_{21}(\hat{x})}{4}, \text{ where } C \in [1, \frac{4}{3}].$$

$h(x)/a > 0$ is violated when $W_e > 10/\kappa$. Our solution therefore has limitations going beyond those involved in the perturbation. Our results here are purely formal and lack rigor.

A formula for the ratio of the final radius of the jet to the pipe radius can be obtained by substituting $\hat{x} = \infty$ in (1.5). Thus

$$\frac{h_f}{a} = 1 + \kappa [0.126 + 0.008 R_e + \phi w_e] - 0.159 \kappa^2 + O(|\bar{u}|^3), \quad (1.6)$$

where $0.272 < \phi < 0.331$. The first two terms on the right-hand side of expression (1.6) are very close to the results

$$h_f/a = 1 + 0.123 \kappa + O(\bar{u}^2) \quad (1.7)$$

obtained analytically by Trogdon and Joseph [4] for the linearized “stick-slip” problem. Trogdon and Joseph [5] also show that (1.7) is a good approximation when $\kappa < 0.1$. Thus we can reasonably expect our results to be valid for a slightly different range of κ . The exact validity domain for this work, however, remains an open question.

2. Mathematical formulation

We consider an axisymmetric extrudate swell problem, illustrated by Fig. 1, in which the lengths L_1, L_2 are extended to infinity. The free surface of the jet is described by the function $h(x; \epsilon)$; and the fluid-filled space is defined

by:

$$V_\epsilon = \{(r, \theta, x) : r \in [0, a], \theta \in [0, 2\pi], x \leq 0\} \\ \cup \{(r, \theta, x) : r \in [0, h(x; \epsilon)], \theta \in [0, 2\pi], x > 0\}, \quad (2.1)$$

where ϵ is a perturbation parameter defined by (2.13). The governing equations of the fluid flow are

$$\nabla \cdot \mathbf{U}(x; \epsilon) = 0 \quad (2.2)$$

and

$$\rho \mathbf{U} \cdot \nabla \mathbf{U} = \text{div } \mathbf{T}, \quad \text{for } x \in V_\epsilon, \quad (2.3)$$

where $\mathbf{T} = -p\mathbf{1} + \mathbf{S}$.

\mathbf{T} is the stress and \mathbf{S} is the extra stress. Our analysis is based on a perturbation of rest state ($\epsilon = 0$) and is carried to order two in ϵ . To this order it suffices, without losing generality in the choice of a constitutive equation, to assume the second-order perturbation of the stress for slow steady flow. Thus

$$\mathbf{S} = \mu \mathbf{A}_1 + \alpha_1 \mathbf{A}_2 + \alpha_2 \mathbf{A}_1^2, \quad (2.4)$$

where

$$\mathbf{A}_1 = \nabla \mathbf{U} + (\nabla \mathbf{U})^T, \\ \mathbf{A}_2 = \mathbf{U} \cdot \nabla \mathbf{A}_1 + \mathbf{A}_1 \cdot \nabla \mathbf{U} + (\mathbf{A}_1 \cdot \nabla \mathbf{U})^T. \quad (2.5)$$

The boundary conditions associated with (2.2–3) are as follows:

(i) There is no-slip along the rigid wall ($r = a, x \leq 0$),

$$\mathbf{U}(a, x; \epsilon) = \mathbf{0}. \quad (2.6)$$

(ii) The free surface is a stream line ($r = h(x; \epsilon), x > 0$),

$$w(h, x; \epsilon) - h'u(h, x; \epsilon) = 0, \quad (2.7)$$

where w and u are the radial and axial velocity components, respectively.

(iii) On the free surface ($r = h(x; \epsilon), x > 0$), the shear stress component T_{nr} vanishes:

$$h'(T_{rr} - T_{xx}) - h'^2 T_{xr} + T_{xr} = 0, \quad (2.8)$$

and the normal stress component T_{nn} is balanced by surface tension

$$T_{rr} - h'T_{xr} - \frac{\sigma h''}{(1 + h'^2)^{3/2}} + \frac{\sigma}{h(1 + h'^2)^{1/2}} = 0. \quad (2.9)$$

The primes in (2.7–9) are derivatives with respect to x at a fixed ϵ ; that is,

$$(\cdot)'(x; \epsilon) \equiv \frac{d}{dx}(\cdot). \quad (2.10)$$

(iv) At the exit plane, the free surface joins the exit lip, so that

$$h(0; \epsilon) = a. \quad (2.11)$$

(v) Far downstream, the flow in the jet is uniform; and the slope of the free surface is flat:

$$h'(x; \epsilon) = 0 \text{ as } x \rightarrow \infty. \quad (2.12)$$

The perturbation parameter ϵ is chosen to be proportional to the volume flow rate Q :

$$\epsilon = \frac{Q}{2\pi} = \int_0^h ur \, dr. \quad (2.13)$$

When $\epsilon = 0$, the above problem has a unique solution (see [6]):

$$[U, p, h] = [\mathbf{0}, \sigma/a, a], \quad (2.14)$$

and $V_\epsilon = V_0$ is an infinite straight tube of radius a .

When $\epsilon \neq 0$, we seek the coefficients through order ϵ^2 of the formal series representation of solutions

$$\begin{bmatrix} U(r, x; \epsilon) \\ p(r, x; \epsilon) \\ h(x; \epsilon) \end{bmatrix} = \begin{bmatrix} \mathbf{0} \\ \sigma/a \\ a \end{bmatrix} + \sum_{n=1}^{\infty} \epsilon^n \begin{bmatrix} U^{[n]}(R, X) \\ p^{[n]}(R, X) \\ h^{[n]}(R, X) \end{bmatrix} \quad (2.15)$$

The coefficients of the series are defined on V_0 . The domain V_ϵ can be determined from the map $V_0 \rightarrow V_\epsilon$:

$$\begin{aligned} r &= \frac{Rh}{a}(x; \epsilon) \\ \theta &= \theta, \\ x &= X. \end{aligned} \quad (2.16)$$

The mapping function (and its series representation) is a to-be-determined unknown of the problem. The coefficients $(\cdot)^{[n]}(R, X)$ of ϵ^n in (2.15) are defined as follows:

$$(\cdot)^{[n]}(R, X) = \frac{1}{n!} \left(\frac{d}{d\epsilon} \right)^n (\cdot)(\mathbf{x}(X; \epsilon); \epsilon) \Big|_{\text{holding } X \text{ fixed}, \epsilon=0}.$$

Another type of coefficients $(\cdot)^{\langle n \rangle}(R, X)$, which is useful for the analysis (see Joseph and Fosdick [9]) is defined in terms of partial derivatives of ϵ

$$(\cdot)^{\langle n \rangle}(R, X) = \frac{1}{n!} \left(\frac{\partial}{\partial \epsilon} \right)^n (\cdot)(\mathbf{x}; \epsilon) \Big|_{\text{holding } \mathbf{x} \text{ fixed}, \epsilon=0}.$$

Relations between the above coefficients can be established using the chain

rule

$$(\cdot)^{[n]}(R; X) = \frac{1}{n!} \left(\frac{\partial}{\partial \epsilon} + \frac{dr}{d\epsilon} \frac{\partial}{\partial r} \right)^n (\cdot)(r, x; \epsilon) \Big|_{x=X, \epsilon=0}, \quad (2.17)$$

where $dr/d\epsilon = h^{[1]}(X) = h^{\langle 1 \rangle}(X)$ at $R = a$.

2.1. The first-order problem

At first order, we obtain a Stokes flow problem defined by:

$$\nabla \cdot \mathbf{U}^{\langle 1 \rangle}(\mathbf{X}) = 0, \quad (2.18)$$

$$-\nabla p^{\langle 1 \rangle}(\mathbf{X}) + \mu \nabla^2 \mathbf{U}^{\langle 1 \rangle}(\mathbf{X}) = 0, \quad \text{for } \mathbf{X} \in V_0. \quad (2.19)$$

The ("stick-slip") boundary conditions on $R = a$ are:

$$\text{at } x \leq 0: \quad w^{\langle 1 \rangle} = u^{\langle 1 \rangle} = 0; \quad (2.20)$$

$$\text{at } x > 0: \quad w^{\langle 1 \rangle} = 0, \quad (2.21)$$

$$\text{and } T_{XR}^{\langle 1 \rangle} = \mu \left[\frac{\partial u^{\langle 1 \rangle}}{\partial R} + \frac{\partial w^{\langle 1 \rangle}}{\partial X} \right] = 0. \quad (2.22)$$

Equations (2.18–19, 20–22) are derived from 2.2–3, 6–8), respectively.

The choice of ϵ in (2.13) leads us to the following conditions at $x = \pm \infty$:

$$\text{As } X \rightarrow -\infty, \quad \int_0^a u^{\langle 1 \rangle} R \, dR = 1; \quad (2.23)$$

$$\text{and as } X \rightarrow \infty, \quad \mathbf{u}^{\langle 1 \rangle} = (2/a^2) \mathbf{e}_x. \quad (2.24)$$

The first-order correction $h^{\langle 1 \rangle}(X)$ is determined by the differential equation

$$h^{\langle 1 \rangle}{}''(X) + \frac{h^{\langle 1 \rangle}(X)}{a^2} = \frac{1}{\sigma} \left[-p^{\langle 1 \rangle}(a, X) + 2\mu \frac{\partial w^{\langle 1 \rangle}}{\partial R}(a, X) \right], \quad (2.25)$$

subject to the boundary conditions:

$$h^{\langle 1 \rangle}(0) = 0. \quad (2.26)$$

$$h^{\langle 1 \rangle}|_{x \rightarrow \infty} = 0. \quad (2.27)$$

The dimensions of $[\epsilon, \mu, \sigma]$ are $[L^3/S, M/LS, M/S^2]$. We use these scales to form the following dimensionless quantities:

$$\hat{x} = X/a,$$

$$\hat{r} = R/a,$$

$$\hat{\nabla} = a\nabla = \mathbf{e}_{\hat{x}} \frac{\partial}{\partial \hat{x}} + \mathbf{e}_{\hat{r}} \frac{\partial}{\partial \hat{r}} + \mathbf{e}_{\hat{\theta}} \frac{1}{\hat{r}} \frac{\partial}{\partial \hat{\theta}},$$

$$\hat{h}_1(\hat{x}) = \frac{a\sigma}{\mu} h^{(1)}(X)$$

$$\hat{p}_1(\hat{r}, \hat{x}) = \frac{a^3}{\mu} p^{(1)}(R, X),$$

$$\hat{U}_1(\hat{r}, \hat{x}) = a^2 U^{(1)}(R, X). \quad (2.28)$$

We also let $\hat{V}_0 \equiv \{(\hat{r}, \theta, \hat{x}) : \hat{r} \in [0, 1], \theta \in [0, 2\pi], -\infty < \hat{x} < \infty\}$. The first-order problem, defined by (2.18–27), can be written in dimensionless form, using (2.28). The resulting dimensionless equations are listed below:

$$\nabla \cdot \hat{U}_1 = 0, \quad (2.29)$$

$$-\hat{\nabla} \hat{p}_1 + \hat{\nabla}^2 U_1 = \mathbf{0}, \text{ in } \hat{V}_0. \quad (2.30)$$

$$\text{For } \hat{x} \leq 0: \hat{w}_1(1, \hat{x}) = \hat{u}_1(1, \hat{x}) = 0; \quad (2.31)$$

$$\text{as } \hat{x} \rightarrow -\infty, \int_0^1 \hat{u}_1 \hat{r} \, d\hat{r} = 1. \quad (2.32)$$

$$\text{For } \hat{x} > 0: \hat{w}_1(1, \hat{x}) = \frac{\partial \hat{u}_1}{\partial \hat{r}}(1, \hat{x}) + \frac{\partial \hat{w}_1}{\partial \hat{x}}(1, \hat{x}) = 0; \quad (2.33)$$

$$\text{as } \hat{x} \rightarrow +\infty, \hat{u}_1 \rightarrow 2. \quad (2.34)$$

The dimensionless free surface correction $\hat{h}_1(\hat{x})$ at first order is given by the solution of

$$\hat{h}_1'' + \hat{h}_1 = -\hat{p}_1 + 2 \frac{\partial \hat{w}_1}{\partial \hat{r}} \text{ for } \hat{x} > 0, \quad (2.35)$$

$$\text{satisfying } \hat{h}_1(0) = \hat{h}_1'|_{\hat{x} \rightarrow \infty} = 0. \quad (2.36)$$

2.2 The second-order problem

The governing equations at second order are

$$\nabla \cdot U^{(2)} = 0, \quad (2.37)$$

$$\rho U^{(1)} \cdot \nabla U^{(1)} = -\nabla p^{(2)} + \mu \nabla^2 U^{(2)} + \nabla \cdot \{ \alpha_1 A_2 [U^{(1)}] + \alpha_2 A_1 [U^{(1)}]^2 \}, \quad (2.38)$$

for $X \in V_0$. Moreover, since

$$\nabla p^{(1)} = \mu \nabla \cdot A_1 [U^{(1)}],$$

it follows from a theorem of Giesekus [12] that

$$\nabla \cdot \{ A_2 [U^{(1)}] - A_1 [U^{(1)}]^2 \} = \nabla \left\{ \frac{U^{(1)}}{\mu} \cdot \nabla p^{(1)} + \frac{1}{4} \text{Tr} \{ A_1 [U^{(1)}]^2 \} \right\}.$$

The equation (2.38) then becomes

$$\rho \mathbf{U}^{(1)} \cdot \nabla \mathbf{U}^{(1)} = \nabla \left\{ -p^{(2)} + \frac{\alpha_1}{\mu} \mathbf{U}^{(1)} \cdot \nabla p^{(1)} + \frac{\alpha_1}{4} \text{Tr} \{ \mathbf{A}_1 [\mathbf{U}^{(1)}]^2 \} \right\} + \mu \nabla^2 \mathbf{U}^{(2)} + (\alpha_1 + \alpha_2) \nabla \cdot \{ \mathbf{A}_1 [\mathbf{U}^{(1)}]^2 \}. \quad (2.39)$$

The governing equation (2.37, 39) satisfy the following boundary conditions:

(i) In the tube, $X \leq 0$,

$$w^{(2)}(a, X) = u^{(2)}(a, X) = 0. \quad (2.40)$$

$$(ii) \text{ As } X \rightarrow -\infty, \int_0^a u^{(2)} R \, dR = 0. \quad (2.41)$$

(iii) In the jet, $X > 0$,

$$w^{(2)} + h^{(1)} \frac{\partial w^{(1)}}{\partial R} - h^{(1)} U^{(1)} = 0, \quad (2.42)$$

$$\frac{\partial u^{(2)}}{\partial R} + \frac{\partial w^{(2)}}{\partial X} + h^{(1)} \frac{\partial}{\partial R} \left(\frac{\partial u^{(1)}}{\partial R} + \frac{\partial w^{(1)}}{\partial X} \right) + 2h^{(1)} \left(\frac{\partial w^{(1)}}{\partial R} - \frac{\partial u^{(1)}}{\partial X} \right) + \frac{\alpha_1}{\mu} \mathbf{A}_{2XR} + \frac{\alpha_2}{\mu} \{ \mathbf{A}_1^2 \}_{XR} = 0. \quad (2.43)$$

(iv) As

$$X \rightarrow +\infty, \quad \mathbf{U}^{(2)} = -\frac{4}{a^3} h_{(\infty)}^{(1)} \mathbf{e}_x. \quad (2.44)$$

The asymptotic conditions (2.41 and 2.44) at $X = \pm \infty$ arise from the choice of ϵ in (II.13), while the conditions (2.40, 42, 43) arise from (2.6–8), respectively.

At positions far upstream from the exit ($X \ll 0$), the velocity at first order is essentially that of Poiseuille flow:

$$\mathbf{U}^{(1)}(R, X) = \mathbf{U}^{*(1)}(R) = 4(1 - R^2) \mathbf{e}_x.$$

The convective term $\rho \mathbf{U}^{*(1)} \cdot \nabla \mathbf{U}^{*(1)}$ vanishes. Equation (2.39) is of the form

$$-\nabla p^{(2)} + \mu \nabla^2 \mathbf{U}^{(2)} = \nabla \gamma(R), \quad (2.45)$$

where $\gamma(R) = 64[\alpha_1(3R^2 - 1) + \frac{3}{2}\alpha_2 R^2]$. The asymptotic problem at $X \ll 0$, is therefore defined by (2.37, 45), subject to the no-slip condition (2.40) and the constraint (2.41). The solution of this problem is

$$\mathbf{U}^{*(2)} = \mathbf{0} \quad (2.46)$$

and $p^{*(2)} = \gamma(R) + \text{constant}$.

For simplicity, we will use the asymptotic boundary condition (2.46.a), when $X \rightarrow -\infty$, instead of the constraint (2.41), in solving the second order problem defined by (2.37, 39) and the boundary conditions (2.40–44).

The free surface correction $h^{(2)}(X)$ at second order can be found by solving the ordinary differential equation

$$\begin{aligned} \sigma \left[h^{(2)''} + \frac{h^{(2)}}{a^2} \right] = & -p^{(2)} + 2\mu \frac{\partial w^{(2)}}{\partial R} + \alpha_1 A_{2RR} + \alpha_2 \{A_1^2\}_{RR} + \\ & + h^{(1)} \frac{\partial}{\partial R} \left(-p^{(1)} + 2\mu \frac{\partial w^{(1)}}{\partial R} \right) \\ & - h^{(1)} \mu \left(\frac{\partial w^{(1)}}{\partial X} + \frac{\partial u^{(1)}}{\partial R} \right) \\ & - \sigma \left\{ \frac{(h^{(1)'})^2}{a} - \frac{h^{(1)2}}{a^3} \right\} \text{ for } X > 0, \end{aligned} \quad (2.47)$$

Subject to boundary conditions

$$h^{(2)}(0) = 0, \quad (2.48)$$

and

$$h^{(2)}|_{X \rightarrow \infty} = 0. \quad (2.49)$$

Equations (2.47–49) are derived from (2.9, 11 and 12).

Some simplifications may be made on the undisturbed jet surface. Since the following boundary condition at first order,

$$w^{(1)} = \frac{\partial w^{(1)}}{\partial X} + \frac{\partial u^{(1)}}{\partial R} = 0,$$

holds at $R = a$ and $X > 0$, it can be shown that terms proportional to $\{A_2\}_{XR}$ and $\{A_1^2\}_{XR}$ in eqn. (2.43) vanish. The term $h^{(1)'} \mu \left(\frac{\partial w^{(1)}}{\partial R} + \frac{\partial u^{(1)}}{\partial X} \right)$ in eqn. (2.47) also vanishes. Furthermore, in this equation we may express the partial derivative $\partial p^{(1)}/\partial R$ using (2.19), as follows:

$$\frac{\partial p^{(1)}}{\partial R} = \mu \left(\frac{\partial^2 w^{(1)}}{\partial R^2} + \frac{1}{R} \frac{\partial w^{(1)}}{\partial R} - \frac{w^{(1)}}{R^2} \right) = \mu \left(\frac{\partial^2 w^{(1)}}{\partial R^2} + \frac{1}{a} \frac{\partial w^{(1)}}{\partial R} \right).$$

We have therefore the equivalence

$$h^{(1)} \frac{\partial}{\partial R} \left(-p^{(1)} + 2\mu \frac{\partial w^{(1)}}{\partial R} \right) = \mu h^{(1)} \left(\frac{\partial^2 w^{(1)}}{\partial R^2} - \frac{1}{a} \frac{\partial w^{(1)}}{\partial R} \right).$$

To form dimensionless equations at second order we use (2.28) and intro-

duce the following dimensionless variables and parameters:

$$\begin{aligned}\hat{h}_2(\hat{x}) &\equiv \frac{a^3 \sigma^2}{\mu^2} h^{(2)}(X), \\ \hat{p}_2(\hat{r}, \hat{x}) &\equiv \frac{a^5 \sigma}{\mu^2} p^{(2)}(R, X), \\ \hat{U}_2(\hat{r}, \hat{x}) &\equiv \frac{a^4 \sigma}{\mu} U^{(2)}(R, X),\end{aligned}\tag{2.50}$$

$$c_0 = \frac{\rho a \sigma}{\mu^2}, \quad c_1 = \frac{\alpha_1 \sigma}{a \mu^2}, \quad c_2 = \frac{\alpha_2 \sigma}{a \mu^2}.\tag{2.51}$$

The dimensionless problem at second order is therefore in the form:

$$\begin{aligned}\hat{\nabla} \cdot \hat{U}_2 &= 0, \\ -\hat{\nabla} \hat{p}_2 + \hat{\nabla}^2 U_2 &= c_0 \hat{U}_1 \cdot \hat{\nabla} \hat{U}_1 - c_1 \hat{\nabla} \left\{ \hat{U}_1 \cdot \nabla \hat{p}_1 + \frac{1}{4} \text{Tr} \{ \hat{A}_1^2 \} \right\} \\ &\quad - (c_1 + c_2) \hat{\nabla} \cdot \{ \hat{A}_1^2 \},\end{aligned}\tag{2.52}$$

for $\hat{x} \in \hat{V}_0$;

$$\left. \begin{aligned}\hat{w}_2 &= - \left[\hat{h}_1 \frac{\partial}{\partial \hat{r}} \hat{w}_1 - \hat{h}'_1 \hat{u}_1 \right], \\ \frac{\partial \hat{w}_2}{\partial \hat{x}} + \frac{\partial \hat{u}_2}{\partial \hat{r}} &= - \left[\hat{h}_1 \frac{\partial}{\partial \hat{r}} \left(\frac{\partial \hat{u}_1}{\partial \hat{r}} + \frac{\partial \hat{w}_1}{\partial \hat{x}} \right) + 2 \hat{h}'_1 \left(\frac{\partial \hat{w}_1}{\partial \hat{r}} - \frac{\partial \hat{u}_1}{\partial \hat{x}} \right) \right], \\ \text{when } \hat{r} &= 1 \text{ and } \hat{x} > 0; \\ \hat{w}_2 = \hat{u}_2 &= 0, \text{ when } \hat{r} = 1 \text{ and } \hat{x} \leq 0; \\ \hat{U}_2|_{\hat{r} \rightarrow -\infty} &= \mathbf{0}; \text{ and} \\ \hat{U}_2|_{\hat{r} \rightarrow +\infty} &= -4 \hat{h}_1 e_x.\end{aligned}\right\} \tag{2.52.cont.}$$

The dimensionless jet shape correction $\hat{h}_2(\hat{x})$, at second order, is determined from the solution of the differential equation

$$\left. \begin{aligned}\hat{h}_2'' + \hat{h}_2 &= -\hat{p}_2 + 2 \frac{\partial}{\partial \hat{r}} \hat{w}_2 + c_2 \{ \hat{A}_1^2 \}_{\hat{r}\hat{r}} + c_1 \hat{A}_{2\hat{r}\hat{r}} \\ &\quad + \hat{h}_1 \left[\frac{\partial^2}{\partial \hat{r}^2} \hat{w}^{(1)} - \frac{\partial}{\partial \hat{r}} \hat{w}^{(1)} \right] - (\hat{h}_1'^2 - \hat{h}_1^2),\end{aligned}\right\} \tag{2.53}$$

for $\hat{x} > 0$, subject to the boundary conditions

$$\hat{h}_2(0) = 0, \quad \text{and } \hat{h}'_2|_{\hat{x} \rightarrow \infty} = 0.$$

Since the problems (2.52) and (2.53) are linear, we have the following decomposition

$$\begin{bmatrix} \hat{\mathbf{U}}_2 \\ \hat{\rho}_2 \\ \hat{h}_2 \end{bmatrix} = \sum_{i=0}^3 c_i \begin{bmatrix} \hat{\mathbf{U}}_{2i} \\ \hat{\rho}_{2i} \\ \hat{h}_{2i} \end{bmatrix}, \quad (2.54)$$

where the coefficient c_i , $i = 0, 1, 2$, are defined by (2.51), and $c_3 = 1$.

(2.55)

The four sets of components $[\hat{\mathbf{U}}_{2i}, \hat{\rho}_{2i}, \hat{h}_{2i}]$, $i = 0, 1, 2, 3$, can then be obtained by solving four sets of problems which arise from (2.52, 53), when terms with coefficients c_0, c_1, c_2 , and unity are collected. These four sets of problems, listed below, are in parameter free form.

$$\left. \begin{aligned} \hat{\nabla} \cdot \hat{\mathbf{U}}_{20} &= 0, \\ \hat{\nabla}^2 \hat{\mathbf{U}}_{20} - \hat{\nabla} \hat{\rho}_{20} &= \hat{\mathbf{U}}^{(1)} \cdot \hat{\nabla} \hat{\mathbf{U}}^{(1)}, \text{ in } \hat{V}_0; \\ \hat{w}_{20} &= \frac{\partial \hat{u}_{20}}{\partial \hat{r}} + \frac{\partial \hat{w}_{20}}{\partial \hat{x}} = 0 \text{ along } \hat{r} = 1 \text{ and } \hat{x} > 0, \\ \hat{w}_{20} &= \hat{u}_{20} = 0 \text{ along } \hat{r} = 1 \text{ and } \hat{x} \leq 0, \\ \hat{\mathbf{U}}_{20}|_{|\hat{x}| \rightarrow \infty} &= \mathbf{0}; \end{aligned} \right\} \quad (2.56.A)$$

$$\left. \begin{aligned} \hat{h}'_{20} + \hat{h}_{20} &= -\hat{\rho}_{20} + 2 \frac{\partial}{\partial \hat{r}} \hat{w}_{20} \text{ along } \hat{r} = 1 \text{ and } \hat{x} > 0, \\ \text{such that } \hat{h}_{20}(0) &= \hat{h}_{20}|_{\hat{x} \rightarrow \infty} = 0. \end{aligned} \right\} \quad (2.56.B)$$

$$\left. \begin{aligned} \hat{\nabla} \cdot \hat{\mathbf{U}}_{21} &= 0, \\ \hat{\nabla}^2 \hat{\mathbf{U}}_{21} - \hat{\nabla} \hat{\rho}_{21} &= -\hat{\nabla} \{ \hat{\mathbf{U}}_1 \cdot \hat{\nabla} \hat{\rho}_1 + \frac{1}{4} \text{Tr} \{ \hat{\mathbf{A}}_1^2 \} \} - \hat{\nabla} \cdot \{ \hat{\mathbf{A}}_1^2 \}, \text{ in } \hat{V}_0; \\ \hat{w}_{21} &= \frac{\partial \hat{u}_{21}}{\partial \hat{r}} + \frac{\partial \hat{w}_{21}}{\partial \hat{x}} = 0 \text{ along } \hat{r} = 1 \text{ and } \hat{x} < 0, \\ \hat{w}_{21} &= \hat{u}_{21} = 0 \text{ along } \hat{r} = 1 \text{ and } \hat{x} \leq 0, \\ \hat{\mathbf{U}}_{21}|_{|\hat{x}| \rightarrow \infty} &= \mathbf{0}; \end{aligned} \right\} \quad (2.57.A)$$

$$\left. \begin{aligned} \hat{h}'_{21} + \hat{h}_{21} &= -\hat{\rho}_{21} + 2 \frac{\partial}{\partial \hat{r}} \hat{w}_{21} + \{ \hat{\mathbf{A}}_2 \}_{\hat{r}\hat{r}} \text{ along } \hat{r} = 1 \text{ and } \hat{x} > 0, \\ \text{such that } \hat{h}_{21}(0) &= \hat{h}'_{21}|_{\hat{x} \rightarrow \infty} = 0. \end{aligned} \right\} \quad (2.57.B)$$

$$\left. \begin{aligned} \hat{\nabla} \cdot \hat{\mathbf{U}}_{22} &= 0, \\ \hat{\nabla}^2 \hat{\mathbf{U}}_{22} - \hat{\nabla} \hat{p}_{22} &= -\hat{\nabla} \cdot \{\hat{\mathbf{A}}_1^2\}, \text{ in } \hat{V}_0; \\ \hat{w}_{22} &= \frac{\partial \hat{u}_{22}}{\partial \hat{r}} + \frac{\partial \hat{w}_{22}}{\partial \hat{x}} = 0 \text{ along } \hat{r} = 1 \text{ and } \hat{x} = 0, \\ \hat{w}_{22} &= \hat{u}_{22} = 0 \text{ along } \hat{r} = 1 \text{ and } \hat{x} \leq 0, \\ \hat{\mathbf{U}}_{22}|_{\hat{x} \rightarrow \infty} &= \mathbf{0}; \end{aligned} \right\} \quad (2.58.A)$$

$$\left. \begin{aligned} \hat{h}'_{22} + \hat{h}_{22} &= -\hat{p}_{22} + 2 \frac{\partial}{\partial \hat{r}} \hat{w}_{22} + \{\hat{\mathbf{A}}_1^2\}_{\hat{r}\hat{r}} \text{ along } \hat{r} = 1 \text{ and } \hat{x} > 0, \\ \text{such that } \hat{h}_{22}(0) &= \hat{h}'_{22}|_{\hat{x} \rightarrow \infty} = 0. \end{aligned} \right\} \quad (2.58.B)$$

$$\left. \begin{aligned} \hat{\nabla} \cdot \hat{\mathbf{U}}_{23} &= 0, \\ \hat{\nabla}^2 \hat{\mathbf{U}}_{23} - \hat{\nabla} \hat{p}_{23} &= \mathbf{0}, \text{ in } \hat{V}_0; \\ \frac{\partial \hat{u}_{23}}{\partial \hat{r}} + \frac{\partial \hat{w}_{23}}{\partial \hat{x}} &= - \left[\hat{h}_1 \frac{\partial}{\partial \hat{r}} \left(\frac{\partial \hat{u}_1}{\partial \hat{r}} + \frac{\partial \hat{w}_1}{\partial \hat{x}} \right) + 2 \hat{h}'_1 \left(\frac{\partial \hat{w}_1}{\partial \hat{r}} - \frac{\partial \hat{u}_1}{\partial \hat{x}} \right) \right], \\ \hat{w}_{23} &= - \left[\hat{h}_1 \frac{\partial \hat{w}_1}{\partial \hat{r}} - \hat{h}'_1 \hat{u}_1 \right], \text{ along } \hat{r} = 1 \text{ and } \hat{x} > 0, \\ \hat{w}_{23} &= \hat{u}_{23} = 0 \text{ along } \hat{r} = 1 \text{ and } \hat{x} \leq 0, \\ \hat{\mathbf{U}}_{23}|_{\hat{x} \rightarrow \infty} &= -4 \hat{h}_1 e_x, \text{ and } \hat{\mathbf{U}}_{23}|_{\hat{x} \rightarrow -\infty} = \mathbf{0}; \end{aligned} \right\} \quad (2.59.A)$$

$$\left. \begin{aligned} \hat{h}'_{23} + \hat{h}_{23} &= -\hat{p}_{23} + 2 \frac{\partial}{\partial \hat{r}} \hat{w}_{23} + \hat{h}_1 \left[\frac{\partial^2}{\partial \hat{r}^2} \hat{w}_1 - \frac{\partial}{\partial \hat{r}} \hat{w}_1 \right] - [\hat{h}'_1{}^2 - \hat{h}_1^2] \\ \text{for } \hat{x} > 0, \text{ such that } \hat{h}_{23}(0) &= \hat{h}'_{23}|_{\hat{x} \rightarrow \infty} = 0. \end{aligned} \right\} \quad (2.59.B)$$

In summary, we have derived five sets of equations and boundary conditions which are to be satisfied by $(\hat{\mathbf{U}}_i, \hat{p}_i, \hat{h}_i)$ and $(\hat{\mathbf{u}}_{2i}, \hat{p}_{2i}, \hat{h}_{2i})$, $i = 0, \dots, 3$. The stick-slip problem defined by (2.39–34), is the first to be solved; and the free surface correction $\hat{h}_1(\hat{x})$ at first order is next determined from (2.35–36). Once $(\hat{u}_1, \hat{p}_1, \hat{h}_1)$ are known, they are substituted into problems (2.56–59) which are in turn to be solved for $(\hat{\mathbf{u}}_{2i}, \hat{p}_{2i}, \hat{h}_{2i})$, $i = 0, 1, 2, 3$. The numerical methods used in computing these solutions will be described in the next section.

3. Numerical solutions

3.1. Velocity and pressure fields

The governing equations for the velocity and pressure fields at first- and second-order problems may be written in the form:

$$\nabla \cdot \tilde{\mathbf{T}} = \mathbf{f}, \quad (3.1)$$

$$\nabla \cdot \mathbf{U} = 0, \text{ in } \hat{V}_0, \quad (3.2)$$

where

$$\tilde{\mathbf{T}} = -p\mathbf{1} + (\nabla\mathbf{U} + (\nabla\mathbf{U})^T) \quad (3.3)$$

and

$$\begin{aligned} p(r, x) &= \tilde{p}(r, x) - \tilde{p}(r, \infty) \\ &= \tilde{p}(r, x) - \tilde{p}_\infty. \end{aligned} \quad (3.4)$$

We want to obtain an approximate solution for $\mathbf{U} = w\mathbf{e}_r + u\mathbf{e}_x$ and $p(r, x)$ in the form

$$u(r, x) = u^* + \sum_{i=1}^N \Phi_i(r, x)u_i,$$

$$w(r, x) = w^* + \sum_{j=1}^M \Phi_j(r, x)w_j,$$

and

$$p(r, x) = \sum_{k=1}^L \psi_k(r, x)p_k. \quad (3.5a-c)$$

u^* , w^* are particular solutions satisfying essential boundary conditions (e.g. prescribed velocity data). The $\Phi_i(r, x)$ are trial functions expressed in global coordinates $(r, x) \in \hat{V}_0$; they form a basis in which the velocity components u , w can be interpolated. A function Φ_i attains unity at its corresponding nodal point (r_i, x_i) and vanishes at any other nodal points. It then follows that

$$w(r_i, x_i) = w_i \text{ and } u(r_i, x_i) = u_i.$$

The trial functions $\psi_k(r, x)$ for the pressure p can be formed in a similar fashion.

We solve (3.1–2) by the Galerkin method. A detailed description for the Galerkin method can be found in [7,13,14]. In our work, the domain \hat{V}_0 is discretized by Lagrangian rectangular elements with 9 nodes for velocities

and 4 nodes for pressure. The velocity trial functions are biquadratic Lagrangian polynomials, and pressure trial functions are bilinear. When the velocities and pressures are known, we compute the forcing functions on the right sides of the surface equations (2.25, 2.56–59, B). Solutions of these equations are given in the following section.

3.2. Residual pressures and surface shape corrections

The ordinary differential equations in (2.25, 2.56–59, B) together with their boundary conditions are of the form:

$$\frac{d^2}{dx^2} Y(x) + Y(x) = \mathcal{F}(x) + \mathcal{F}_\infty, \quad (3.6)$$

$$Y(x) = 0, \text{ at } x = 0, \quad (3.7)$$

$$\frac{d}{dx} Y = 0, \text{ as } x \rightarrow \infty, \quad (3.8)$$

where

$$\mathcal{F}(x) = 0, \text{ as } x \rightarrow \infty.$$

Given the differential operator on the left of (3.6) together with the boundary conditions (3.7), (3.8), one cannot choose \mathcal{F}_∞ independent of the variation $\mathcal{F}(x)$. To prove this we note that the general solution of (3.6) is

$$Y(x) = A \sin x + B \cos x + \int_0^x (\mathcal{F}(\xi) + \mathcal{F}_\infty) \sin(x - \xi) d\xi. \quad (3.9)$$

Condition (3.7) requires $B = 0$.

Differentiating (3.9) with respect to x , we get

$$Y'(x) = A \cos x + \int_0^x (\mathcal{F}(\xi) + \mathcal{F}_\infty) \cos(x - \xi) d\xi.$$

Using the identity $\cos(x - \xi) = \cos x \cos \xi + \sin x \sin \xi$ in the above equation, we obtain

$$Y'(x) = \left(A + \int_0^x \mathcal{F}(\xi) \cos \xi d\xi \right) \cos x + \left(\mathcal{F}_\infty + \int_0^x \mathcal{F}(\xi) \sin \xi d\xi \right) \sin x.$$

To satisfy (3.8), one must have

$$\mathcal{F}_\infty = - \int_0^\infty \mathcal{F}(\xi) \sin \xi d\xi, \quad (3.10)$$

and

$$A = - \int_0^\infty \mathcal{F}(\xi) \cos \xi d\xi.$$

The general solution is thus reduced to

$$Y(x) = \mathfrak{F}_\infty - \int_x^\infty \mathfrak{F}(\xi) \sin(x - \xi) d\xi. \quad (3.11)$$

Since for sufficiently large x^* , $\mathfrak{F}(x) = 0$ for $x \geq x^*$, it is possible to obtain a numerical estimate for \mathfrak{F}_∞ and $Y(x)$ from the relations

$$\mathfrak{F}_\infty = - \int_0^{x^*} \mathfrak{F}(\xi) \sin \xi d\xi, \quad (3.12)$$

$$Y(x) = \mathfrak{F}_\infty - \int_x^{x^*} \mathfrak{F}(\xi) \sin(x - \xi) d\xi. \quad (3.13)$$

Computations are essentially carried out for four meshes which are drawn to scale in Fig. 8. The pipe and jet lengths in these meshes are roughly $L_1 = L_2 = 2$. Results obtained with these four meshes are stable as the grid is refined at the exit lip. Computations with other meshes where larger pipe and jet lengths L_1, L_2 are used, show that all of the surface shape corrections, except $\hat{h}_{23}(\hat{x})$, nearly attain at $\hat{x} = 2$ their asymptotic values (at $\hat{x} = \infty$). For example, using mesh V which is just mesh I with extra elements added to increase L_2 to 3.6, we find that $h_{23}(\hat{x} = 3.6) = 2.54$ compared with $h_{23}(\hat{x} = 2) = 2.25$ as suggested by meshes I–IV. The variations of the asymptotic values of the surface shape corrections with the mesh are depicted in Fig. 9.

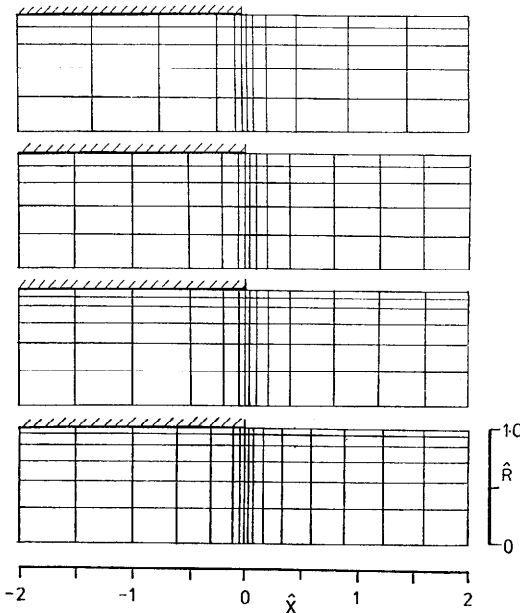


Fig. 8. The meshes used in computations of solutions for perturbation problems.

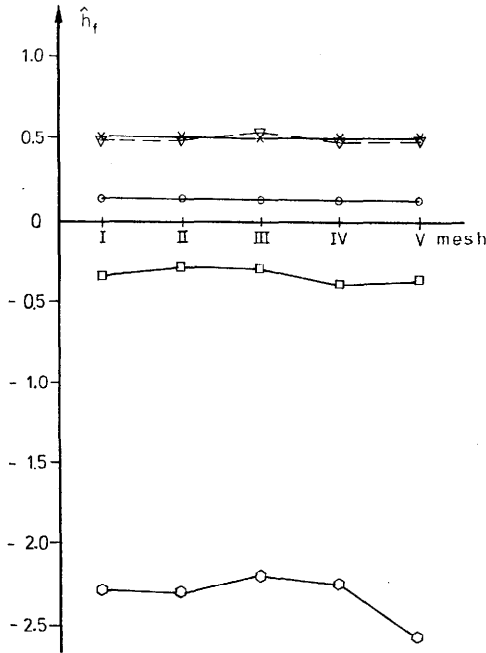


Fig. 9. Variations of final surface shape corrections with the mesh.

\hat{h}_1 ×; \hat{h}_{20} ○; \hat{h}_{21} □; \hat{h}_{22} ▽; \hat{h}_{23} ◇.

References

1. M.J. Crochet and R. Keunings, *J. Non-Newtonian Fluid Mech.*, 10 (1982) 339.
2. L.D. Sturges, *J. Non-Newtonian Fluid Mech.*, 9 (1981) 357.
3. D.D. Joseph, *Arch. Rational Mech. Anal.*, 74 (1983) 389.
4. S.A. Trogdon and D.D. Joseph, part I, *Rheol. Acta*, 19 (1980) 404.
5. S.A. Trogdon and D.D. Joseph, part II, *Rheol. Acta*, 20 (1981) 1.
6. A.C. Pipkin and R.I. Tanner, *Mechanics Today*, Vol. 1, Pergamon Press, Oxford, 1972, p. 262.
7. H.A. Tieu, Ph.D. Thesis, University of Minnesota, 1983.
8. C. Truesdell and W. Noll, *The Non-Linear Field Theories of Mechanics*, Volume III/3, Springer-Verlag, Berlin-Heidelberg-New York, 1965, p. 455.
9. D.D. Joseph and R.L. Fosdick, part I, *Arch. Rational Mech. Anal.*, 49 (1973) 321.
10. J.C. Saut and D.D. Joseph, *Fading Memory*, *Arch. Rational Mech. Anal.*, 81 (1983) 53.
11. D.D. Joseph, *Arch. Rational Mech. Anal.*, 56 (1974) 99.
12. H. Giesekus, *Rheol. Acta*, 3 (1963) 59.
13. G. Strang and G.J. Fix, *An Analysis of the Finite Element Method*, Prentice-Hall, Inc., Englewood Cliffs, NJ, 1973.
14. D.C. Zienkiewicz, *The Finite Element Method*, third ed., McGraw-Hill, 1977.